ICREN-01/2012 December 15-16, 2012 Constantine, Algeria
First International Conference on Renewable Energies and Nanotechnology impact on Medicine and Ecology

Numerical Prediction of a Turbulent Separated Flow Using a CFD Code

Boukhadia Karima[a], Bouzidane Ahmed[b], Hammou Mahmoud[c]

[a]*Mechanical Engineering faculty Department of Mechanical engineering, University of Sciences and Technology Mohamed Boudiaf U.S.T.Oran Algeria*
[b, c] *Faculty of Science and Technology and Materials Science Department of Mechanical Engineering, Ibn Khaldun University Tiaret Algeria*

Abstract

In the present study, the subsonic flow in an asymmetrical diffuser was simulated numerically using code CFX 11.0 and its generator of grid ICEM CFD. Two models of turbulence were tested: K- ε and K- ω SST.
The results obtained showed that the K- ε model singularly over-estimates the speed value close to the wall and that the K- ω SST model is qualitatively in good agreement with the experimental results of Buice and Eaton 1997. They also showed that the separation and réattachement of the fluid on the tilted wall strongly depends on its angle of inclination and that the length of the zone of separation increases with the angle of inclination of the lower wall of the diffuser
Keywords: Asymmetric diffuser, Separation, Reattachment, Tilt angle, Separation zone.

I. Introduction

At the outing of heat engines, recuperation of lost kinetic energy on form of heat is done by a type of divergent conduit called diffuser. Diffusers are integral parts in fuel injection engines and much of other devices that depend on the flow of fluid. The performances of a propulsion system as a whole depend on the effectiveness of diffusers.

Identification of the separation of flow in diffusers is significant since separation increases the trail and causes the deformation of ventilators and compressors of engines.

Simulation of flow in diffusers is a task particularly of defies for CFD due to unfavorable pressure gradient created by the deceleration of flow, which frequently results the separations.

These separations depend strongly on the level of turbulence, the viscous effects of walls, and on the pressure ratio of the diffuser, which are functions of the speed gradient and the physical geometry. Thus, the modeling of turbulence and geometry became dominant factors that affect the capacity of the CFD to envisage exactly flows crossing diffusers.

The aim of this work is to contribute to a field of research, which relates study of the separate turbulent flow in diffusers through commercial code CFX 11.0 by using two models of turbulence : k-ε and k-ω SST.

Nomenclature

C_f	Friction coefficient	
C_p	Pressure coefficient	
C_μ, $C_{\varepsilon\iota}$	Constants of the *k-ε* model	(ι=1;2)
CFD	Computational fluid dynamics	
fi	Gravity force	[N]
g	Gravity	[m/s2]
H	Height of outing of diffuser	[m]
k	Kinetic turbulent energy	[J.kg-1]
l	Scale of turbulent length	[m]
M	Mach number	
P	Pressure	[Pa]
P_k	Production of kinetic turbulent energy	[kg /m.s3]
Re	Reynolds number	(Re = ρ.U.x / μ)
Ut	Parallel wall speed	[m/s]
$u^+ \equiv \frac{U^*}{U} = f(y^+)$	Speed near wall	[m/s]
x, y, z	Cartesian Coordinats	[m]
$y^+ = \frac{y_* U^* \rho_w}{\mu_w}$	Adimensional distance normal on wall	
$U^* = \sqrt{\tau_w / \rho_w}$	Friction speed on wall	
u, v, w	Speed components	[m/s]
Δy	Normal distance on solid wall	[m]
μ	Dynamic viscosity	[Pa.s]
τ_w	Shear wall stress	[kg/m².s²]

$y^+ = \frac{y_* U^* \rho_w}{\mu_w}$	Adimensionnel distance normal on wall	
$U^* = \sqrt{\tau_w / \rho_w}$	Friction speed on wall	
u, v, w	Speed components	[m/s]
Δy	Normal distance on solid wall	[m]
μ	Dynamic viscosity	[Pa.s]
τ_w	Shear wall stress	[kg/m².s²]

II. Flow through diffusers

Tunnel of air used for the experiment is shown on fig 1. The air enters on tunnel through a vein provided with a filter and leaves the ventilator in a small expansion room followed by the diffuser with two additional grids; the grids are designed to ensure a homogeneous flow on the entry of diffuser and to decrease pressure to avoid separation in the diffuser.

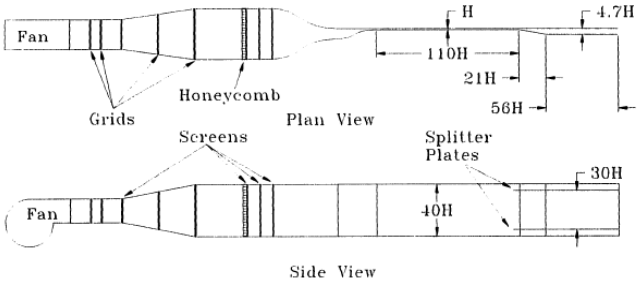

Fig. 1. Air tunnel with test section of the asymmetrical diffuser.

The height of channel H is 1.5 cm ; it has been selected to provide a length of admission of 110H (165 cm) in order to ensure the whole development of the flow in the channel in the inlet of diffuser; and an elongation of 40 H in the admission of channel to provide the two-dimensionality of flow in the channel.

The geometric shape of diffuser has an asymmetric expansion to a total report of surface of 4.7 and a distance of 21H, giving an angle of diffuser approximately 10 degrees. Transitions between parallel and inclined walls have a radius of 9.7 H. The section of conduit is about 56 H and continues until the beginning of flow in the room.

III.1 Formulation of problem

The asymmetric 2d diffuser (fig 2), in which the turbulent flow is two-dimensional, incompressible and without transfer of heat (air with 25°C), entirely developed, undergoes a separation and a reattachement close to the tilted lower wall to the bottom with various angles.

The lower wall of diffuser of Buice and Eaton opens the diffuser with 4.7 times the height of entry H (H = 0.59055 In), the flow in the diffuser is roughly in Mach=0.058.

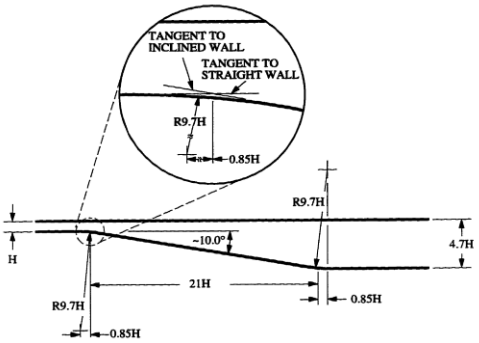

Fig. 2. Detailed geometry of diffuser.

The field of calculation consists of:

- Inlet part height H, and 110 H length, which represents the entry of flow.
- A divergent part with a varying angle of inclination from 6 to 14, and of length 21 H.
- and the outlet part height 4.7 H and of length 65 H ;

The junction of lower surfaces of different parts is carried out with arcs of circles of ray R = 9.7 H, H=14.9997 mm (0.59055 Inch).

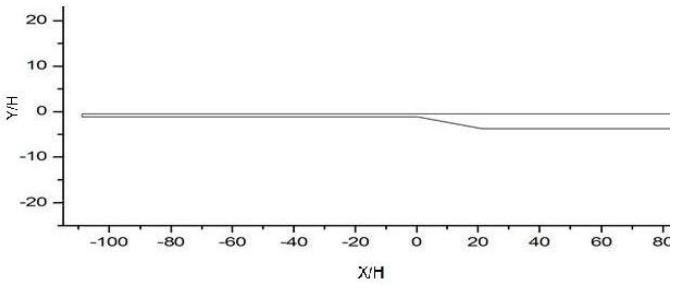

Fig. 3. Illustration of the geometrical configuration of diffuser.

III.2 Modeling flow in diffusers

Flow in a diffuser is three-dimensional, viscous and turbulent, it is completely described by the Navier-Stokes equations which we associate the equation of state of the considered fluid.

In practical applications, certain simplifying assumptions, associated considerations on the geometry and the energy balances are however introduced in order to simplify these equations and to work out simple models for the calculation of the flows.

In the studies of conception and forecast of the performances of diffusers, the flow is supposed adiabatic and two-dimensional. Thermodynamic properties of fluid flow are defined along a middle line of flow and are specified only in entry and to the exit.

Equations modeling the incompressible flow in a diffuser expresses the principles of conservation of mass and the quantity of movement. In Cartesian coordinates (x, y), these equations ere written in stationary regime as following:

$$\frac{\partial u}{\partial \mathrm{x}}+\frac{\partial v}{\partial \mathrm{y}}=0$$

$$\frac{\partial u}{\partial t}+\mathrm{u}\frac{\partial u}{\partial \mathrm{x}}+\mathrm{v}\frac{\partial u}{\partial \mathrm{y}}=-\frac{1}{\rho}\frac{\partial p}{\partial x}+\nu\left(\frac{\partial^2 u}{\partial \mathrm{x}^2}+\frac{\partial^2 u}{\partial \mathrm{y}^2}\right)$$

$$\frac{\partial v}{\partial t}+\mathrm{u}\frac{\partial v}{\partial \mathrm{x}}+\mathrm{v}\frac{\partial v}{\partial \mathrm{y}}=-\frac{1}{\rho}\frac{\partial p}{\partial y}+\nu\left(\frac{\partial^2 v}{\partial \mathrm{x}^2}+\frac{\partial^2 v}{\partial \mathrm{y}^2}\right)$$

III.3 Boundary conditions

- *The entry of fluid(inlet)*

Speed at the entry of diffuser corresponds to a Reynolds number equal to 20000.
For $\mathrm{x}=-110\mathrm{H}$, and $0\geq y\geq H$

- *The exit of fluid (outlet)*

$$\frac{\partial \phi}{\partial \mathrm{x}}=0$$

- *Walls*

A condition of adherence is considered for the lower wall ($-110H\leq x\leq 86H\ H\geq y\geq 4{,}7H$) and the higher wall ($-110H\leq x\leq 86H$ and y=0) $u=v=w=0$

- *Symmetry*

Surfaces of right side and left are defined like symmetry:

$$\frac{\partial u}{\partial z}=0 \qquad w=0 \qquad \frac{\partial v}{\partial z}=0$$

VI.1 Presentation of CFD code

ICEM CFD is a mailler which allows to prepare the geometrical configuration and to generate the tétrahédral and hexahédral grid in a rather convivial way although enough complexes.

CFX Pre; Preprocessor makes possible to define the physical problem as well as boundary conditions of the physical field of flow.

The CFX Solver, which solves the equations modeling the physical problem.

VI.2 Assumptions

For turbulent flows, CFX permits to use the two classic categories of models based on the concept of the turbulent viscosity and the second order models of closing.

The flow chosen in this study is turbulent two-dimensional, stationary, and incompressible without transfer of heat, and the turbulence models undertaken during simulation are the model K - ε and the K-ω SST model.

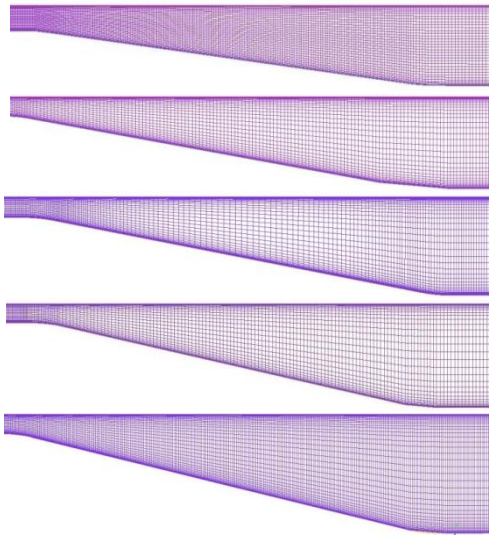

Fig. 4. Grids for different angles of inclination 6,8,10,12 and 14.

VI.3 grid

Several grids with hexahedral elements were tested, (620,633 and 3465 points) according to x and (40 to 50 and 80) points following y and this for each angle of inclination.

VI.4 Sensitivity of grid

Theoretically, errors related to the grid must disappear for more and more fine meshes, until roughly reaching values independent of mesh size. Thus to analyze the quality of grid; three grids were tested (620×40), (633×50) and (3455×81). It is significant to announce that the generated meshes are strongly tightened close to walls. Figs 5, 6 and 7 present the distributions of the friction coefficient C_f and y^+ the along of lower and higher walls of diffuser. A finer analysis of figures shows than starting from the second grid, the use of thinner mesh doesn't generate any considerable variations on the solution.

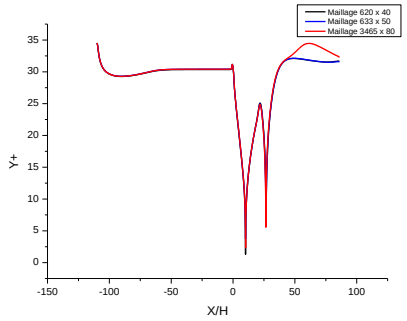

Fig. 5. Distribution de y+ sur la paroi inferieure, diffuseur à 10°.

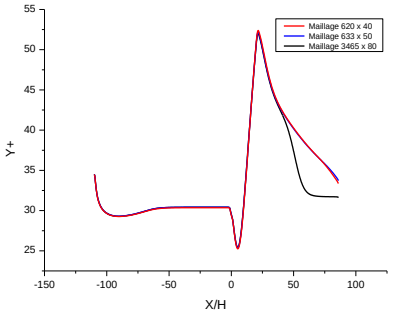

Fig. 6. Distribution de y+ sur la paroi supérieure, diffuseur à 10°.

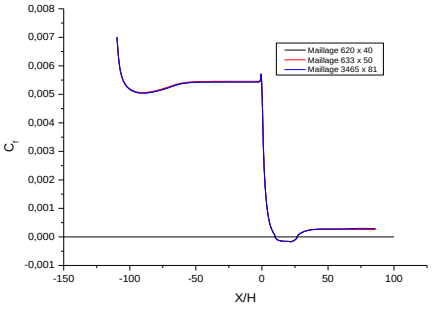

Fig. 7. Distribution de Cf sur la paroi inférieure, diffuseur à 10°.

The grid of (633×50) has been adopted for all simulations. The quality of the grid has also been verified by the values of y^+ that are consisted between 30 and 60. They approach of the requisite y^+ value to the level of the under viscous layer for this type of flow.

When turbulent flow exists, the viscous shear effort is also present that can be added to τ_t. The all shear effort of the turbulent flow is thus

$$\tau = \rho.(\nu + \varepsilon).\frac{dU}{dy}$$

ε is not a property of the fluid as ν, it depends on several factors such as the Reynolds number of flow and of turbulence level, its value is generally much larger than ν .

The empirical relations near wall are known, the following relation gives the friction coefficient

$$C_f = \tau_w / \frac{1}{2}.\rho.U_m^2$$

Where

U_m is the mean velocity of flow.

In the turbulent flow

$$4\,C_f = \frac{0.316}{(Re_d)^{1/4}}$$

This empirical formula of the loss load ratio is made for smooth surfaces; its value will increase if surface is rough.

CFX-Post uses speed along x direction to calculate this friction coefficient C_f. Since diffuser is locked up, the best proceeded was necessary to calculate the friction coefficient of wall. A program was written to calculate speed, in the diverged part of diffuser named block U_{bulk} through entry of calculation field. The U_{bulk} speed was calculated by:

$$U_{bulk} = \frac{\sum_{j=2}^{n-1}\left(U_j.\frac{1}{2}.(y_{j+1}-y_{j-1})\right)}{\sum_{j=2}^{n-1}\frac{1}{2}.(y_{j+1}-y_{j-1})}$$

n is the number of points vertically through the diffuser. Consequently, the friction coefficient for each point along the lower wall was calculated by:

$$C_{f_{lower}} = \frac{U_2/(y_2-y_1)}{\frac{1}{2}.\rho.U_{bulk}}$$

ρ is the air density.

By the same way, the friction coefficient along the upper wall was calculated according to the following formula:

$$C_{f_{upper}} = \frac{u_{n-1}/(y_n-y_{n-1})}{\frac{1}{2}.\rho.U_{bulk}}$$

V.1 Results and discussion

The results presented relate exclusively distributions of the friction and pressure coefficients, with the profiles speeds, the threads of flow and contours of the turbulent kinetic energy inside diffuser. Results were confronted with those of Buice and Eaton's diffuser which is a test case frequently met for the validation of the simulating codes.

The higher and lower walls are placed as solid walls. The inlet fluid is given as an arbitrary fluid with a total air temperature of 25 °C. The outlet boundary is considered a free exit border of fluid; and right and left surfaces are defined like symmetry. Two models of turbulence are tested : the K-ε model and the K-ω SST model.

Fig 8 illustrates speed profiles at different axial positions in the diffuser corresponding to the two turbulence models tested. The obtained results show that the qualitative form of the calculated profiles is well appropriate with experimental data and that the model K-ε singularly over-estimates the speed value close near to wall and that the model K-ω SST is qualitatively in good agreement with the experimental results of Buice and Eaton.

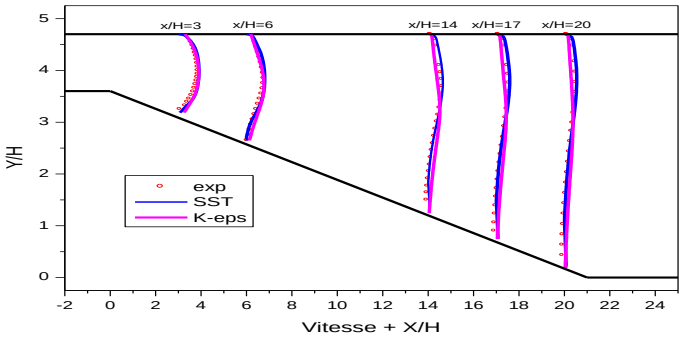

Fig. 8. Speed profiles of diffuser with 10° of inclination.

It is wise to notice also that the K-ω model seems to be more appropriate for calculation of negative speed values close to lower wall to diffuser. The K-ε model does not well catch the detachment of flow. The turbulent flow entirely developed at the inlet of diffuser, is subjected to a strong unfavorable pressure gradient, turbulence in this sudden case undergoes fast changes.

The aerodynamic effects of whirlwind that appear at the entry of the diffuser affect considerably the flow in this area; distribution of the pressure coefficient along the lower wall (fig 9) confirms this result, flow is aspired to the entry under an effect of an unfavorable pressure gradient.

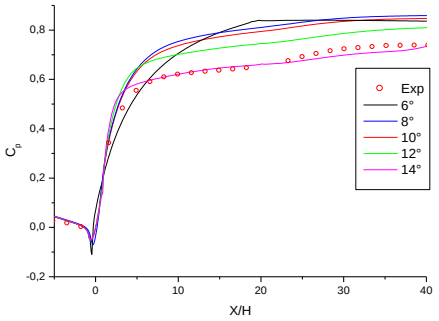

Fig. 9. Pressure coefficient on the lower wall for different angles, speed of flow of 30 m/s. ¶

The reduced area noted on convex surface at the entry of the diffuser represents separation and the presence of this area was confirmed by the experiment of Buice and Eaton (1997).

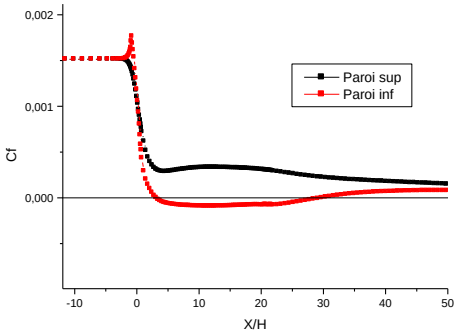

Fig. 10. Friction coefficient on the upper and lower wall of the diffuser of 10°.

The point of separation is easily captured (fig 10), the friction of the right wall in the diffuser decreases quickly in simulation that in the experiment of Buice and Eaton. The speed profiles are fuller than in the experiment close to the right wall at the exit of the channel, this can also be seen in the Cf curve, because the flow of the exit of channel develops into profiles of flow, the friction coefficients of the walls roughly approach to 2 x 10-3.

By traversing the diffuser for upstream to downstream, the flow remains attached to the two walls until a large bubble of separation is formed on the tilted wall (fig 11). The results obtained by PIV (for case 10) give an average point of separation to x/H = 7 in case of Buice and Eaton (1997) 10°. The coefficient of

the reversed flow measured in the experiment of the diffuser with 10 (sometimes called fraction of the reversed flow), shows that the instantaneous inversion of flow occurs on the inclined wall at x/H = 7, the point of réattachement of the average flow was found at the exit at x/H = 28 in the case of Buice and Eaton diffuser.

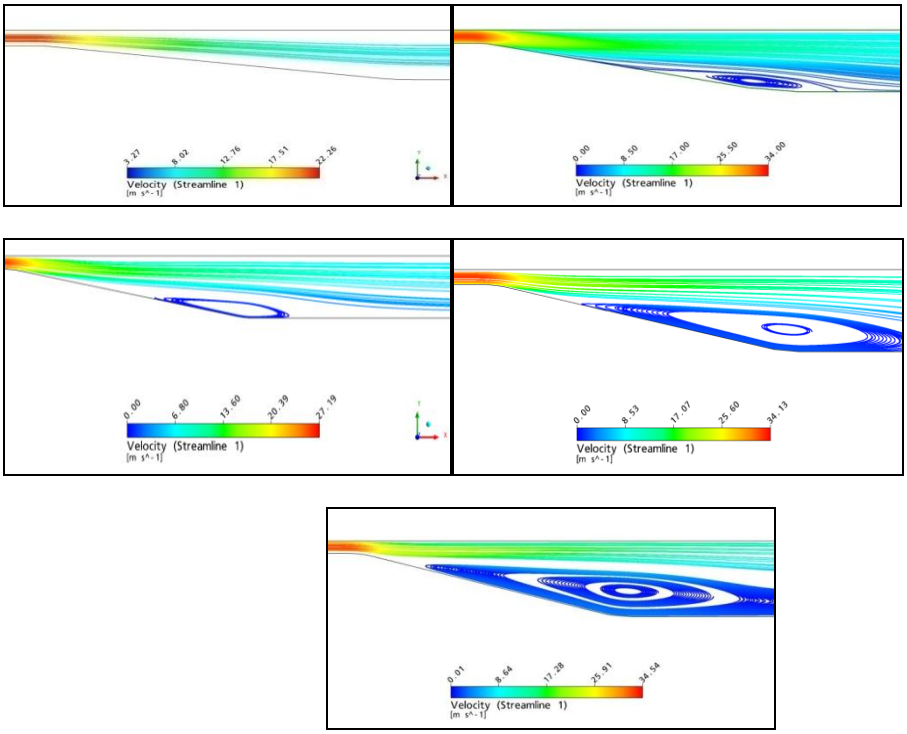

Fig. 11. Formation of the separation bubble close to the tilted wall.

On figs 11, we represents the contour of flow lines in the tilted zone of the diffuser, which shows the recirculation zone of flow, this zone can be a consequence of separation of the flow close to the wall and it explains the negative speeds appearance. The length of separation zone increases with the angle of inclination of the lower wall of each diffuser.

V.2 The average flow

By comparing the size and the shape of the separation bubble of prediction models with experimental results, on fig 12, profiles that separate recirculation zone for the flow close to the wall are represented in the case of 6°, 8° and case of 10°. No experimental data is available for the case of 6° (fig 12.a), but simulation indicates that the size of the separation bubble decreases quickly for angles smaller than 8°. For that, simulations were carried out in the case of angle 6°, and with this angle no area of recirculation was obtained.

In 10° case (fig 12.c), the average point of separation resulting from calculation is almost nearly as in the experiment (Buice and Eaton) and it is difficult to see that on the figure since the separation bubble is very thin close to the point of separation. The point of réattachement calculated is located at x/H = 27.

The full lines show the numerical results and the tear lines show the experimental data.

On fig 12, the height of the separation bubble calculated for case of 8° is roughly 60% of the experiment. The flow predicted by CFX separates from the wall at x/H=7, this calculated bubble is very thin also at 4 H upstream of the measured separation point, the point of réattachement is in agreement and it is located at X/H = 27 and 28 respectively for calculation and the experiment.

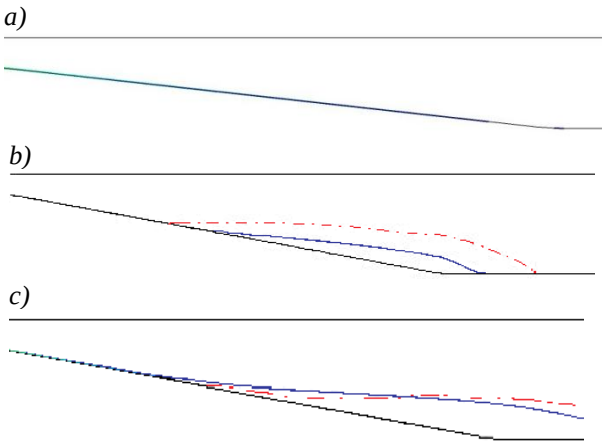

Fig. 12. Profiles that separate the recirculation zone from the average flow for the cases 6°, b) 8° and c) 10°.

V.3 Quantities of turbulence

Since each of the three components speed was measured in the experiment, it is possible to compare the quantities such as the kinetic energy of turbulence, $K = \overline{u_i' u_i'}/2$ or its production rate $\mathcal{P} = \overline{u_i' u_k'}\, \partial U_i / \partial x_k$

The profiles of the kinetic energy (fig 13.a) show a rather good agreement in the higher part of the diffuser, while going towards the downstream, we see that the calculated kinetic energy of turbulence quantities by simulation are small that those measured by the experiment.

The production rate calculated by simulation (fig 13.b), exceeds that's measured in most part of the diffuser, but it has the same quantity as that measured in the exit of the channel. In the upstream part of the diffuser, measurements and calculation agree in general. However, the components of the normal wall on the fig 13.c are larger in simulation and constitute an exception in this respect. We can observe the same behavior in the simulation of case 10°, fig 14.

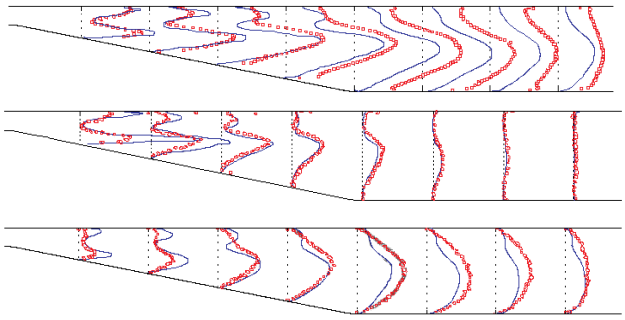

Fig. 13. (o) Experimental data (__) the CFX predictions of turbulence quantities for case 8:
a) turbulent kinetic energy; b) rate production of the turbulent kinetic energy and c) variation of the normal component speed to the wall (direction y) and the tear lines show zero level of each position.

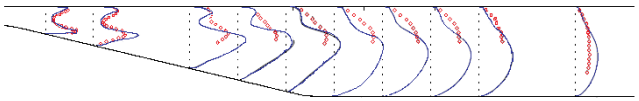

Fig. 14. Variation of the normal speed to the wall for case 10°, (o) experimental data of Buice and Eaton (1997), (_) CFX predictions and tear lines show the zero level of each position.

The length of the separation zone increases with the angle of inclination of the lower wall of each diffuser and the peak of the intensity of the kinetic energy is well captured.

The fluid viscosity is the origin of the dissipation of kinetic energy; this kinetic energy is transformed into intern energy, in absence of contribution of energy (agitation), turbulent kinetic energy decrease quickly in time.

V.4 Effect of inclination

Angle of diffuser	Separation x/H	Reattachement x/H
Experience	7,4	28,2
6°	-	-
8°	11	26
10°	7	27
12°	6	33
14°	4	42

Table 1. Positions of separation and réattachement of fluid along the lower wall.

The results of numerical simulations show that separation and réattachement of fluid on the tilted wall strongly depends on its angle of inclination. The position of the negative Cf (fig 15) indicates the advent of separation. With regard to the angle of inclination of the lower wall, more it is high the point of

separation advances upstream of the diffuser and more the point of reattachement moves back towards the downstream. This situation leads to more losses by pressure and friction. The length of the separation zone increases with the angle of inclination of the lower wall of the diffuser.

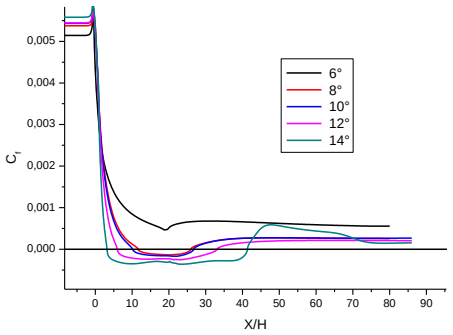

Fig. 15. Distribution of C_f on the lower wall for different angles of inclination.

IV General Conclusion

In the present study, the subsonic flow in an asymmetrical diffuser was simulated numerically through CFX 11.0 code and its generator of grid ICEM CFD. Two models of turbulences were tested: K-ε and K-ω SST.

The results obtained showed that the K-ε model singularly over-estimates the value of speed close to the wall and that the model K-ω SST is qualitatively in good agreement with the experimental results of Buice and Eaton. They also showed that the separation and reattachement of fluid on the tilted wall strongly depends on its angle of inclination and that the length of separation zone increases with inclination angle of the lower wall of diffuser. In prospect, a future study in 3d, appears interesting, and would be judicious to make integrate more sophisticated turbulence models which makes it possible to describe most correctly possible the separate flows.

Bibliographical references ¶

[1] Carl U. Buice "Experimental investigation of flow through an asymmetric plane diffuser" 1997.

[2] Buice, & Eaton, J.K, "Experimental Investigation of Flow Through an Asymmetric Plane Diffuser", Journal of Fluids Engineering, Vol. 122, pp. 433-435, June 2000

[3] Gianluca Iaccarino, "Predictions of a Turbulent Separated Flow Using Commercial CFD Codes", Stanford University, Stanford, 2001

[4] Mauri, S. "Numerical Simulation and flow analysis of an elbow diffuse"r. PhD thesis, EPFL No 2527, 2002

[5] Olle Törnblom, Astrid Herbst & Arne V. Johansson, "Separation control in a plane asymmetric diffuser by means of streamwise vortices experiment, modelling and simulation", Stockholm, Suède. 2004

[6] J.U. Schlüter, "Large-Eddy Simulations of a Separated Plane Diffuser", Stanford University de. 2005

[7] Teryn DalBello "Computational Study of Separating Flow in a Planar Subsonic diffuser"; University of Toled, NASA 2005

[8] Vance Dippold III and Nicholas J. Georgiadis, "Computational Study of Separating Flow in a Planar Subsonic Diffuser"; Ohio NASA / 2005